Tractive Force on Surface of River Bank due to Overflow

by

Masanori MICHIUE*, Koichi SUZUKI* and Osamu HINOKIDANI*

* Department of Civil Engineering

(Received August 2, 1984)

Flow properties and tractive force on a river bank slope due to flooding are discussed both for smooth and rough surfaces. Theoretical distribution of the tractive force is calculated by the momentum equation of boundary layer which develops under the accelerated main flow and is verified by the experiments.

1. Introduction

One of the major causes of river bank breakage is flooding. The mechanism of bank erosion by the overflow should be discussed in order to know the strength of the bank against the overflow. And the distribution of tractive force over the bank surface due to the overflow is essentially important in discussing the mechanism of bank erosion. When water flows over a river bank which has a steep slope, the flow is accelerated due to gravity from the top of the bank to some place where the gravity force is balanced with the shear stress of the bank surface. The velocity distribution changes from almost uniform to greatly distibuted in this accelerated flow region, due to the development of a turbulent boundary layer, and also in this region the tractive force on the bank surface changes dramatically. In this paper tractive force and flow properties such as velocity distribution and water surface profiles are discussed on the basis of the boundary layer theory[1], which is also applied for water flow over a spillway from a reservior by Iwasa[2]. And Theoretical results are verified by experiments of model banks both for smooth and rough surface.

2. Theoretical Analysis

2.1 Basic equation

Turbulent boundary layer δ, where velocity gradient is large, develops along the bank slope x from the top of the bank under the main flow where velocity distribution is almost uniform u_o as shown in Fig.1. In the main flow, energy loss can be neglected, i.e. potential energy changes to velocity energy along the flow direction. If total energy head above the top of the bank is expressed by E, the basic equation for the main flow, using notations in Fig.1, is as follows;

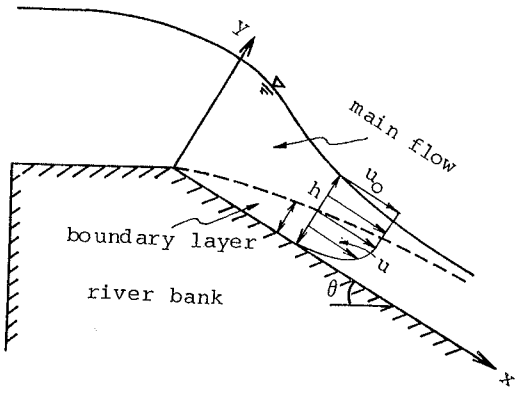

Fig.1 Schematic diagram of flow over a river bank.

$$E\left(\equiv \frac{3}{2}h_c\right) = \frac{u_o^2}{2g} + h\cos\theta - x\sin\theta \qquad (1)$$

where h_c is the critical flow depth, g is the acceleration due to gravity, u_o is the velocity of x direction(along the bank slope), h is the water depth and θ is the slope angle. For the boundary layer where energy loss can not be neglected, equation of momentum will be used as the basic equation of the flow.

$$\frac{\tau_o}{\rho} = g\delta\left(\sin\theta - \cos\theta\frac{dh}{dx}\right) - \frac{d}{dx}\int_0^\delta u^2 dy + u_o\frac{d}{dy}\int_0^\delta u dy \tag{2}$$

where τ_o is the bed shear stress, ρ is the water density, δ is the thickness of the boundary layer, u is the velocity and y is the axis nornal to the bank surface. Putting eq.(1) into eq.(2), one gets the well known von Karman's equation as;

$$\frac{\tau_o}{\rho u_o^2} = \frac{d\vartheta}{dx} + \frac{1}{u_o}\frac{du_o}{dx}(2\vartheta + \delta_*) \tag{3}$$

where δ_* and ϑ are the displacement and momentum thicknesses, respectively and defined as;

$$\delta_* = \frac{1}{u_o}\int_0^\delta (u_o - u)\,dy \quad , \qquad \vartheta = \frac{1}{u_o^2}\int_0^\delta u(u_o - u)\,dy \tag{4}$$

If velocity distribution of the main flow is uniform, water discharge per unit width, q, can be expressed as;

$$q = u_c h_c \equiv \sqrt{g}\, h_c^{3/2} = u_o(h - \delta_*) \tag{5}$$

where u_c is the critical velocity and h_c is the critical water depth which appears at the top of the bank.

2.2 Flow depth and water surface gradient

From eq.(5), one gets

$$u_o = \sqrt{g}\, h_c^{3/2}/(h - \delta_*) \tag{6}$$

and, putting this equation into eq.(1), following equation which expresses the relationship between flow depth h and distance along the x axis can be obtained as;

$$\frac{x}{h_c} = \left\{\left(\frac{h}{h-\delta_*}\right)^2 - 3\left(\frac{h}{h_c}\right)^2 + 2\left(\frac{h}{h_c}\right)^3\cos\theta\right\}/2\left(\frac{h}{h_c}\right)^2\sin\theta \tag{7}.$$

As du_o/dx can be calculated from eq.(6) as;

$$\frac{du_o}{dx} = -\frac{\sqrt{g}\,h_c^{3/2}}{(h-\delta_*)^2}\left(\frac{dh}{dx} - \frac{d\delta_*}{dx}\right) \tag{8},$$

the gradient of water surface can be derived, differentiating eq.(7) by x as follows;

$$\frac{dh}{dx} = \left\{\sin\theta - \frac{h_c^3}{(h-\delta_*)^3}\frac{d\delta_*}{dx}\right\}/\left\{\cos\theta - \left(\frac{h_c}{h-\delta_*}\right)^3\right\} \tag{9}$$

where δ_* and $d\delta_*/dx$ are unknowns but usually $h \gg \delta_*$ and δ_* can be neglected, whereas $d\delta_*/dx$ can not be neglected.

2.3 Bed shear stress

If the velocity profile in the boundary layer is assumed to be the power type

$$\frac{u}{u_0} = \left(\frac{y}{\delta}\right)^n \tag{10}$$

where $0<n<1$, the displacement and momentum thicknesses are obtained by eq. (4) as follows, respectively;

$$\delta_* = \frac{n}{(n+1)}\delta \qquad \vartheta = \frac{n}{(n+1)(2n+1)}\delta \tag{11}.$$

From eqs. (3) and (11), one gets

$$\frac{\tau_0}{\rho u_0^2} = \frac{n}{(n+1)(2n+1)}\frac{d\delta}{dx} + \frac{4n+1}{(n+1)(2n+1)}\frac{\delta}{u_0}\frac{du_0}{dx} \tag{12}.$$

For the boundary layer which develops on a smooth plate with constant main flow velocity (u_0=constant), shear stress on the plate can be expressed in the well-known equation;

$$\frac{\tau_0}{\rho u_0^2} = 0.0225\left(\frac{u_0\delta}{\nu}\right)^{-1/4} \tag{13}$$

where ν is the coefficient of kinematic viscosity. In the case of the flow over a river bank, the main flow is accelerated and eq. (13) can not be applied for the accelerated flow. But by assuming that the effect of acceleration of the main flow is corrected by using eq. (12), eq. (13) is used for the flow over a smooth bank slope for convenience. Then, from eqs. (12) and (13), one can calculate δ as a function of x, using eqs. (1), (6), (8) and (9). Putting $\delta(x)$ into eq. (13), the distribution of the bed shear stress is obtained for a smooth surface.

For a rough bed, $\tau_0/\rho u_0^2$ is a function not only of δ but also bed roughness k and is expressed by the following experimental equation[3] for non-accelerated flow (u_0=constant);

$$\frac{\tau_0}{\rho u_0^2} = 0.0231\alpha - 0.0013 \quad , \qquad \alpha = 0.0844 + 0.3786\left(\frac{k}{\delta}\right)^{1/3} \tag{14}.$$

For convenience, eq. (14) is also applied for the flow over a river bank with rough surface. One can calculate δ as a function of x from eqs. (12) and (14), using eqs. (1), (6), (8) and (9). The distribution of the bed shear stress for the rough bed can be calculated, putting this δ into eq. (14).

3. Experiments and Discussion

3.1 Summary of experiments

A model river bank with a slope of 1:2 and a height of 30cm was settled in a flume 40cm wide and 15m long as shown in Fig.2. Experiments were carried out for a smooth surface slope which was finished by painting, and for a rough surface slope which was covered with sand (diameter of 1.1mm) fixed with vanish. Experimental conditions are shown in Table 1, in which q is the discharge per unit width of the bank and h_c is the critical water depth. Runs S-1 - S-9 are for the smooth surface slope and Runs R-1 - R-9 are for the rough surface slope. Slope of the bank is 1:2, i.e. $\tan\theta=1/2$.

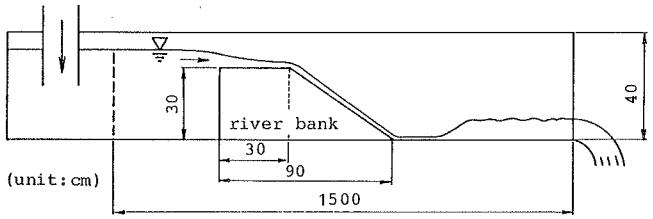

Fig.2 Experimental flume and model bank.

Table 1 Experimental conditions.

Run	q (cm^2/sec)	h_c (cm)	u_c (cm/sec)	$\tan\theta$
S-1	95.46	2.10	45.5	
S-2	106.60	2.26	47.2	
S-3	123.79	2.50	49.5	
S-4	123.93	2.50	49.6	
S-5	143.84	2.76	52.1	1/2
S-6	158.11	2.94	53.8	
S-7	170.34	3.09	55.1	
S-8	195.62	3.39	57.7	
S-9	205.82	3.51	58.6	
R-1	84.83	1.94	43.7	
R-2	96.77	2.12	45.6	
R-3	112.23	2.34	48.0	
R-4	112.97	2.49	49.4	
R-5	138.80	2.70	51.4	1/2
R-6	154.59	2.90	53.3	
R-7	159.94	2.97	53.9	
R-8	177.99	3.19	55.8	
R-9	194.06	3.37	57.6	

Flow velocities were measured by a Pitot tube with a pipe diameter of 1mm, and the pressure difference between dynamic and static pressures was measured electrically by a pressure transducer. Water surface profiles were measured by both point guage and photographs which were taken through a transparent channel wall.

3.2 Water surface profiles

Fig.3(a) and (b) show the relationships between non-dimensional water depth h/h_c and non-dimensional distance x/h_c for smooth and rough surface, respectively. Curves in the figures are calculated by eq.(7) which is derived by neglecting energy loss in the main flow. In the case of the smooth surface, observed data coincide with the calculated curve for almost the entire length of the slope, whereas in the case of rough surface observed water depth does not change for the value of x/h_c more than 10. This means that the main flow on a smooth bed can be assumed not to lose energy for a relatively long distance, but on a rough bed normal depth flow in which bed shear stress and x-component of gravity force are balanced appears in a relatively short distance from the beginning of the slope. When the flow is normal and the Manning's formula is used for the mean

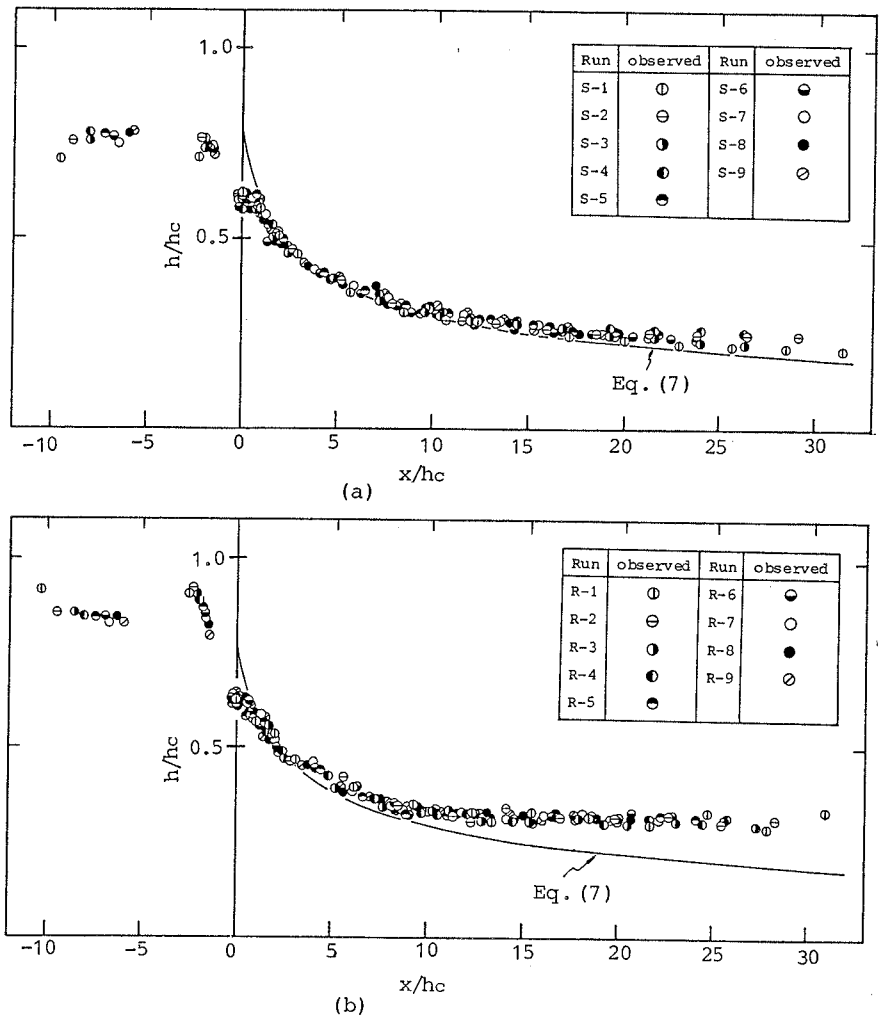

Fig. 3 Water surface profiles ((a) smooth (b) rough).

velocity, the normal flow depth h_o is expressed as;

$$h_o = \left(\frac{n_1^2 q^2}{i} \right)^{3/10} \tag{15}$$

where n_1 is the coefficient of the Manning's roughness and i is the bed slope. Using the Manning-Strickler's formula $k_s^{1/6}/n_1\sqrt{g}=7.66$(units:m,s) which is the relationship between n_1 and the equivalent sand roughness k_s, one gets the following equation from eq. (15);

$$\frac{h_o}{h_c} = \left(\frac{1}{7.66^2 i} \right)^{3/10} \cdot \left(\frac{k_s}{h_c} \right)^{1/10} \tag{16}.$$

As the slope i is 0.447 and k_s is 0.11cm (sand diameter) for the rough surface in the experiments, h_0/h_c changes from 0.335 (Run R-9) to 0.355 (Run R-1). It seems that in the region of $x/h_c > \sim 15$ the flow is almost normal.

3.3 Velocity profiles

Fig.4 shows an example of velocity profiles at several positions x where solid lines are velocity profiles for the smooth bed and dotted lines are for the rough bed. Velocity profiles at points of the value x more than 26 ($x/h_c \simeq 10$) differ much between the rough and smooth beds. The boundary layer thickness is defined as the value of y at $u=0.99u_0$ and it is determined from the velocity profiles such as shown in Fig.4. But the value of δ is not accurate, because it is difficult to find out the exact position y where $u=0.99u_0$.

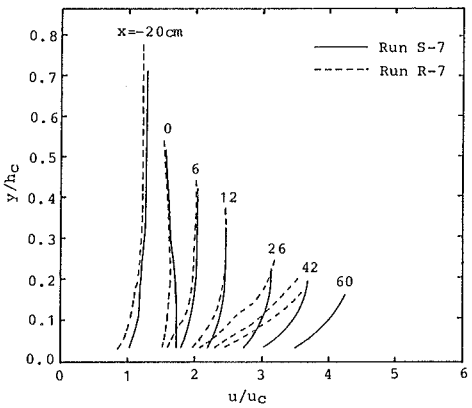

Fig.4 Velocity profiles.

Fig.5 shows the relationships between u/u_0 and y/δ in the boundary layer. In the figure, solid lines are calculated by eq.(10) for $n=1/7$. Because of the inaccuracy of δ, precise discussion about the velocity profiles is impossible. But it seems that the power n in eq.(10) is a little less than 1/7 in the region where the main flow is accelerated and it approaches 1/7 when the flow depth approaches the normal flow depth.

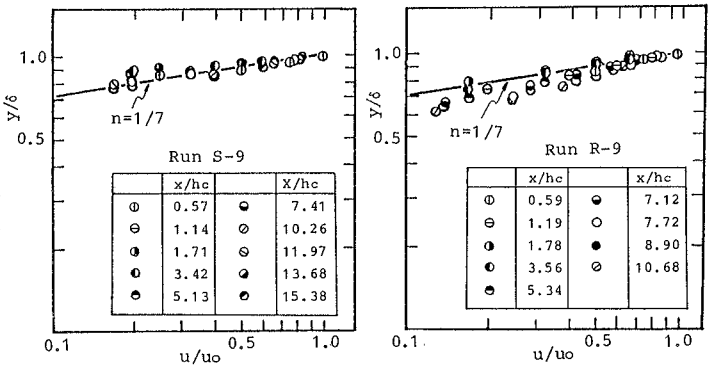

Fig.5 Velocity profiles in boundary layer.

3.4 Distribution of tractive force

Fig.6 and Fig.7 show the distributions of non-dimensional bed shear stress $\tau_0/\rho u_c^2$ along the flow direction x/h_c for the smooth and rough surface beds, respectively. Assuming that the power n in eq.(10) is 1/7 in the case of the smooth surface (Fig.6), one gets the following differential equation (17) from eqs.(12) and (13);

$$\frac{7}{72}\frac{d\delta}{dx} + \frac{23}{72}\frac{\delta}{u_0}\frac{du_0}{dx} = 0.0225\left(\frac{u_0\delta}{\nu}\right)^{-1/4} \qquad (17).$$

Because u_0 in eq.(17) can be calculated by eqs.(6) and (7), assuming $\delta_* \ll h$, theoretical curves in Fig.6 are obtained numerically from eq.(17) under the boundary

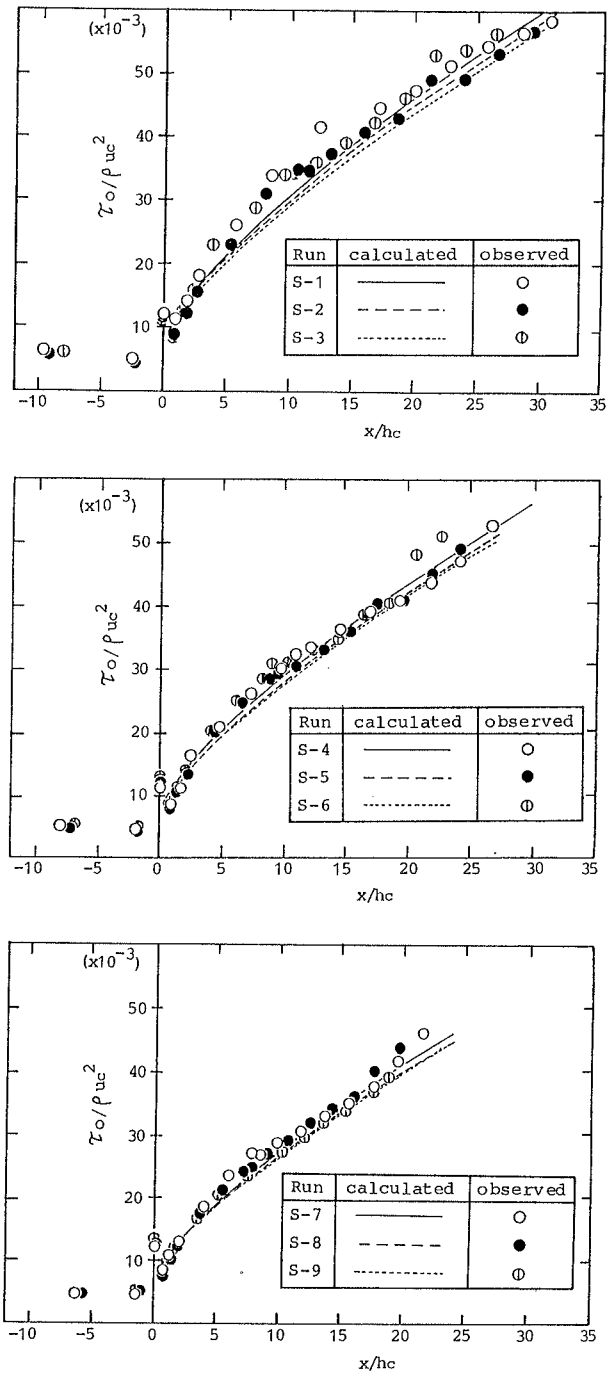

Fig.6 Distribution of non-dimensional tractive force along flow direction (smooth surface).

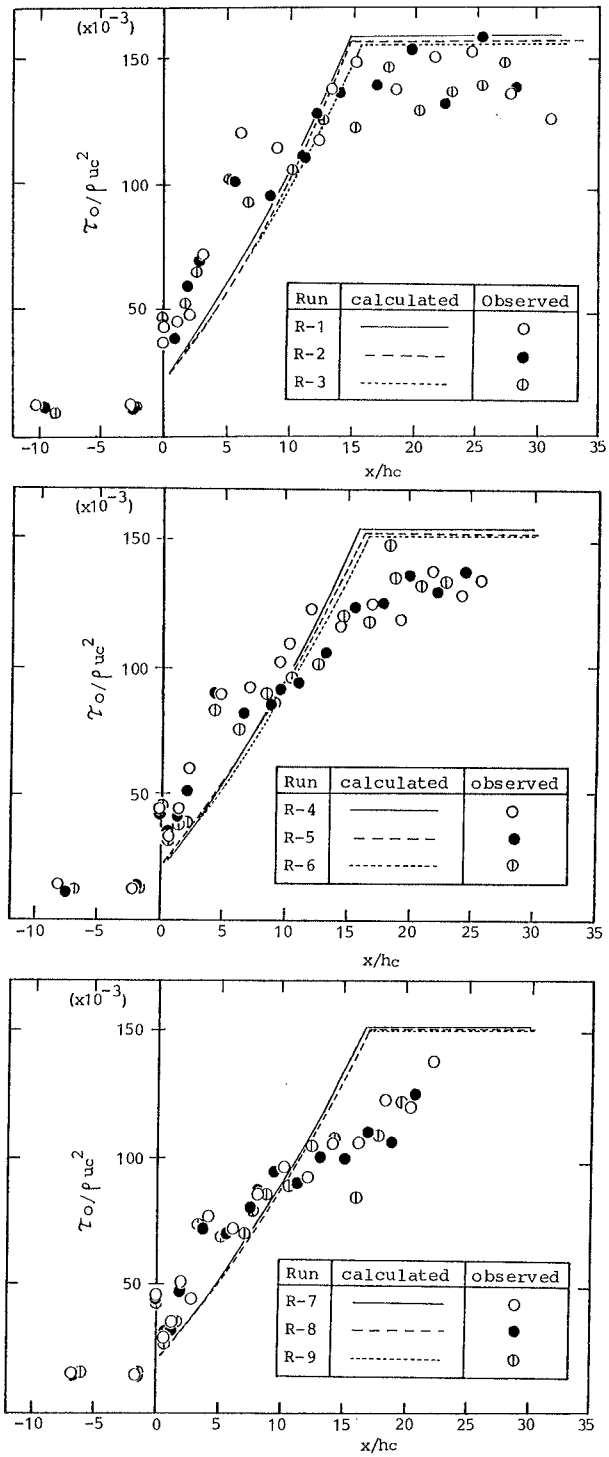

Fig.7 Distribution of non-dimensional tractive force along flow direction (rough surface).

condition that $\delta = h_c/1000 (\simeq 0)$ at $x=0$. Experimental data are obtained by the principle of Preston tube[4], using the measured velocity just near the bed ($y=$ 1.0mm). Theoretical curves are in good agreement with the experimental data and it can be concluded that the bed shear stress on a smooth surface slope can be given by the above mentioned theory. In the case of the rough surface (Fig. 7), the principle of Preston tube can not be applied for calculating the bed shear stress τ_o. Then experimental data in the figures are obtained, using the measured velocity u_b at $y=1.0$mm and the friction factor C_{fn} at the normal flow depth as follows;

$$\tau_o = \frac{1}{2} C_{fn} \rho u_b^2 \ , \quad C_{fn} \left(\equiv \frac{2\tau_{on}}{\rho u_{bn}^2} \right) = \frac{2gh_o i}{u_{bn}^2} \tag{18}$$

where suffix n means the normal flow and C_f at the accelerated flow region is assumed to be equal to C_{fn}. On the other hand, theoretical curves are given in the normal flow region ($x/h_c < \sim 15$) by $\tau_o = \rho g h_o i$, using h_o calculated by eq. (16). And in the accelerated region ($0 < x/h_c < \sim 15$), h_o can be given theoretically, solving the following equation (19) obtained from eq. (12) for $n=1/7$ and eq. (14);

$$\frac{7}{72} \frac{d\delta}{dx} + \frac{23}{72} \frac{\delta}{u_o} \frac{du_o}{dx} = 0.0006 + 0.0087 \left(\frac{k}{\delta} \right)^{1/3} \tag{19}.$$

Theoretical curves coincide with experimental data to some extent except for the transitional region ($\sim 10 < x/h_c < \sim 15$).

4. Conclusion

Distribution of tractive force on a bank slope due to flooding has been given theoretically, solving the momentum equation for the boundary layer whose outer edge velocity is assumed to be accelerated as a potential flow. This theoretical tractive force coincides with the experimental data over almost the entire length of the slope with a smooth surface, but in the case of a rough surface the main flow can be assumed to be potential flow only for a relatively short distance from the beginning of the slope and the flow soon becomes normal, where the tractive force is balanced with the gravity force.

References

1) Schlichting,H.: Boundary-Layer Theory, McGraw-Hill, sixth Edition, 1968.
2) Iwasa,Y.: Boundary layer growth of open channel flow on a smooth bed and its contribution to practical application to channel design, Memories of Faculty of Engineering, Kyoto Univ., Vol.19, No.3, 1957, pp.229-254.
3) Fujimoto,B.: Fluid Mechanics, Yokendo Press, 1968 (in Japanese).
4) Patal,V.C.: Calibration of the Preston tube and limitation on its use in pressure gradients, Jour. of Fluid Mech., Vol.23, 1965, pp.185-208.